



# RAFT agent effect on graft poly(acrylic acid) to polypropylene glycol fumarate phthalate

Akmaral Zh. Sarsenbekova<sup>1</sup> · Gaziza M. Zhumanazarova<sup>1</sup> · Ertan Yildirim<sup>2</sup> · Yerkeblan M. Tazhbayev<sup>1</sup> · Gulshakhar K. Kudaibergen<sup>3</sup>

Received: 14 August 2023 / Accepted: 29 December 2023 / Published online: 24 February 2024  
© The Author(s) 2024

## Abstract

Understanding the physical and chemical properties of new-generation polymeric materials during the synthesis is very important in obtaining the desired product in design and production. Chemical, thermal, and physical parameters as well as degradation kinetics of the resins developed especially in recent years are the main stages that determine the polymer composition process that affects material selection. In this study, the potential to use RAFT agent (2-cyano-2-propyl-dodecyl-trithiocarbonate, CPDT) in the synthesis of new polymers based on polypropylene fumarate phthalate has revealed important properties. To exemplify, the concentration of the RAFT agent affects the polymer-based mesh density associated with the yield of the product. Changes in swelling behavior and thermodynamic parameters of polymers synthesized in the presence of RAFT agent were observed. Chemical composition and stability characterizations of the synthesized grafted polymers were performed by FT-IR, <sup>13</sup>C, <sup>1</sup>H-NMR spectroscopy and TGA. The grafted polymers analyzed by SEM morphology were found to have hydrogel sorption potential showed signs of a loose surface and the formation of a layered and porous structure in comparison with the grafted polymers. The resulting compounds have a high swelling capacity and increased yield. At the same time, this study will shed light on the thermodynamic calculations of the graft polymers in order to determine or predicting the polymer composition.

---

Dedicated to the memory of Meiram Burkeev, who passed away while pursuing his scientific studies.

---

✉ Gaziza M. Zhumanazarova  
gaziza.zhumanazarova@mail.ru

Akmaral Zh. Sarsenbekova  
chem\_akmaral@mail.ru

Ertan Yildirim  
ertan.yildirim@gazi.edu.tr

Yerkeblan M. Tazhbayev  
tazhbaev@mail.ru

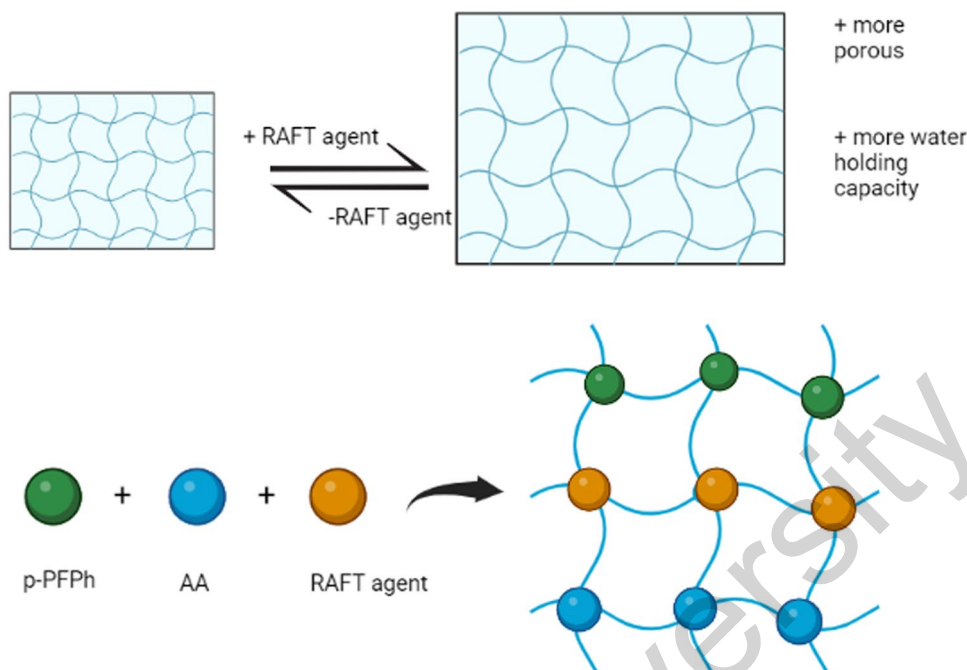
Gulshakhar K. Kudaibergen  
kudaibergen@biocenter.kz

<sup>1</sup> Chemistry Faculty, Karagandy University of the Name of Academician E.A. Buketov, 100024 Karaganda, Kazakhstan

<sup>2</sup> Department of Chemistry, Faculty of Science, Gazi University, 06500 Besevler, Ankara, Turkey

<sup>3</sup> Stem Cell Laboratory, National Center for Biotechnology, 010000 Astana, Kazakhstan

## Graphical abstract



**Keywords** Unsaturated polyester · Polypropylene glycol fumarate phthalate · Acrylic acid · RAFT polymerization

## Introduction

To date, changing the properties of previously known polymers in the production and development of polymeric materials is very important in terms of both material performance and application of the materials. Changes in the properties of known polymeric materials lead to new material properties, but at the same time, the use of extra chemicals is prevented. When evaluated in this context, the development of unsaturated polyester resins with different compositions, especially from previously known materials, has drawn the attention of researchers (Formela et al. 2022; Chen et al. 2019; Yasko et al. 2000).

Unsaturated polyester resins (UPRs) have many applications and advantages. Due to a number of their properties, such as high adhesion, mechanical strength, and chemical resistance properties, UPRs are thermoset polymeric materials used for general purposes in marine, aviation, automotive, electronics, and medicine today. Compared to epoxy resins, lower cost and simple production techniques are important advantages of UPRs (Kandelbauer et al. 2014; Zhao et al. 2018; Baskaran et al. 2011; Naguib and Zhang 2018; Muniyati and Lovell 2007).

UPRs are highly hydrophobic by nature. However, the presence of reactive vinyl bonds in UPRs allows them to easily graft polymerize with hydrophobic vinyl monomers

(vinyl acetate, styrene) and hydrophilic (acrylic and methacrylic acids, acrylamide) monomers (Burkeev et al. 2013, 2015a, 2015b, 2018, 2021a; Sarsenbekova et al. 2019). Thus, new possibilities are opened in the production of smart materials by adding polymeric units with desired properties to UPRs with previously known properties. The process of obtaining the smart material to be designed is directly dependent on the grafted polymer structures to be synthesized. For this reason, it is very important to investigate both the structural and physical properties of the grafted polymers to be synthesized.

In traditional radical polymerizations, limitations such as not being able to control the polymer molecular weight in the synthesized polymers, obtaining polymers with high dispersity, and not following the kinetic process clearly create challenges in understanding the properties of the smart materials to be obtained. Therefore, in order to avoid such restrictions, controlled/living radical polymerization (CRP) techniques have been preferred by researchers in recent years. Controlled/living radical polymerization techniques have advantages such as first-order kinetic behavior, low dispersity, and desired architecture. Most importantly, they have the ability to control the polymerization process (growth of polymer chains, obtaining polymers with desired molecular weights, etc.). Therefore, these techniques enable easy and controlled synthesis of grafted, star-shaped, and block polymers. CRP

techniques are basically known as atom transfer radical polymerization (ATRP), reversible addition-fragmentation chain transfer radical polymerization (RAFT), and nitrogen-mediated polymerization (NMP). In the ATRP technique, one of these techniques, the use of heavy metals (such as copper) and the need for additional processes to remove them are the disadvantages of the technique in terms of both time and cost (Moad and Polymerization 2015; Barner-Kowollik 2008; Chat et al. 2022; Tardy et al. 2017). In the NMP technique, on the other hand, the fact that the polymerization conditions are not mild imposes limitations on industrial processes (Oadian 2004; Ageyeva et al. 2018; Czajka et al. 2022; Ahmadvani et al. 2017). RAFT technique is a class of controlled (living) radical polymerization method that attracts special attention due to its unique ability to control the molecular weight of the polymer, molecular weight distribution, composition, and architecture of polymer chains in mild conditions, and heavy metals are not used in the polymers obtained by this technique (Truong et al. 2021; Xie et al. 2021; Moad et al. 2013; Tanaka et al. 2021; Abbasian et al. 2013, 2015; Mohammad-Rezaei et al. 2018). As a result, RAFT polymerization is an up-to-date technology for the production of new materials with different properties. The main reasons for the choice of the RAFT method are the following indicators. Firstly, the RAFT polymerization process does not require the use of a metal catalyst; secondly, the polymerization process is not limited to strict reaction conditions such as a certain temperature range or the use of a particular solvent (IriSofa et al. 2019; Mahmoodzadeh et al. 2017; Abbasian and Amirmanesh 2017; Tian et al. 2018; Abbasian and Khakpour 2016; Karaj-Abad et al. 2019). The choice of comonomers in RAFT polymerization is not limited either. Thus, comonomers can be used both with and without functional groups ( $-\text{NR}_2$ ,  $-\text{OH}$ ,  $-\text{CONR}_2$ ,  $-\text{COOH}$ ) (Steenberge et al. 2019; Liu et al. 2013; Zhou et al. 2019; Heiny and Shastri 2015; Lee et al. 2018; Muringayil Joseph et al. 2020; Suresh et al. 2022; Tanaka et al. 2023; György and Armes 2023; Clothier et al. 2023). Burkeev et al. synthesized Polypropylene glycol maleate phthalate and acrylic acid grafted polymers using the free radical polymerization technique. Ag and Ni transition metal nanoparticles were immobilized to the synthesized grafted polymers. They obtained information about the catalytic properties of these composites as a result of the electrocatalytic hydrogenation reaction. They investigated the effects of pore size, diameter, and size distribution of metal nanoparticles in grafted polymer matrices synthesized by the free radical polymerization technique. In a grafted polymer based on acrylic acid and polypropylene glycol maleate phthalate, a homogeneous distribution of metal nanoparticles was achieved and aggregation of the particles in the polymer volume was prevented. Thus, the obtained hybrid polymer immobilized Ni and Ag nanoparticles were proven to be effective catalysts

for the hydrogenation of unsaturated compounds (Burkeev et al. 2021b). In a study conducted in 2022, the effect of RAFT agent on the graft polymerization of polypropylene glycol maleate with acrylic acid was investigated. The reaction process of radical graft polymerization of polypropylene glycol maleate with acrylic acid was followed when RAFT agent was used. When RAFT agent was used, the results were evaluated by determining the regularity and characteristics of the polymerization, calculating the composition, and also examining the density of the spatial network of the grafted polymers obtained. It has been determined that the behavior of the synthesized grafted polymers during swelling depends directly on the concentration of the RAFT agent in the polymer composition. In addition, it was concluded that the network structure and product yield of the grafted polymers depend on the concentration of the RAFT agent as well as the comonomers that prevent the disorder in the structure. Therefore, graft polymerization processes using the RAFT agent have the potential to turn them into promising hydrogels, making it possible to obtain grafted polymers with multifunctional properties (Kazhmuratova et al. 2022). In 2023, Zhumanazarova et al. increased the thermal stability of polypropylene glycol fumarate phthalate (p-PFPh) and acrylic acid (AA)-based grafted polymers. They showed that the grafted polymers exposed to high temperatures have stable behavior and that these grafted polymers have the potential to be used as hydrogels for processing vegetable crops. It is also known that the grafted polymerization products of unsaturated polyester resins and vinyl monomers have high melting point and crosslinked grafted polymers with a chaotic grid position in space. The fact that radical grafted polymerization does not allow the full synthesis of grafted polymers with desired properties provides an opportunity to use RAFT polymerization (Sarsenbekova et al. 2023).

RAFT polymerization can offer significant advantages for synthesizing grafted polymers with previously known polypropylene fumarate phthalate. Based on this approach, it may be very interesting to investigate the graft polymerization process based on the superior properties of RAFT polymerization. In the detailed literature research, the effect of RAFT agent on polypropylene glycol maleate and acrylic acid grafted polymer was investigated. At the same time, grafted polymers of polypropylene glycol fumarate phthalate (p-PFPh) and acrylic acid (AA) used in this study were synthesized by free radical polymerization technique. The stability of p-PFPh and AA grafted polymer was investigated only at high temperature by using RAFT agent. In this study, unlike the literature, p-PFPh and AA grafted polymers were synthesized both by free radical polymerization and in the presence of RAFT agent, and detailed characterizations were carried out (Burkeev et al. 2022). According to the results obtained, it has been understood that the grafted polymers obtained in the presence of RAFT agent are more regular,

porous and have higher water absorption capacity than the polymers obtained according to the free radical polymerization technique.

## Experimental part

### Materials

Propylene glycol ( $\geq 99.5\%$ , Atameken chemicals), phthalic anhydride ( $\geq 99\%$ , Sigma-Aldrich), fumaric acid ( $\geq 99.0\%$ , Sigma-Aldrich), zinc chloride ( $\geq 98\%$ , Sigma-Aldrich), acrylic acid ( $\geq 99.5\%$ , Atameken chemicals), benzoyl peroxide (98%, Primechemicals group), 1,4-dioxane ( $\geq 99.5\%$ , Atameken chemicals), and RAFT agent (2-Cyano-2-propyl dodecyl trithiocarbonate, CPDT) (97% (HPLC), Sigma-Aldrich) were used without further purification.

### Synthesis of polypropylene glycol fumarate phthalate

Polypropylene fumarate phthalate (p-PFPh) was obtained by the polycondensation reaction of fumaric acid, phthalic anhydride with propylene glycol, taken in quantities of 0.7:0.3:1.05 mol.

After assembling the working model, the calculated amount of propylene glycol is loaded into a four-neck flask and heated to 30–40 °C, then bulk reagents (fumaric acid and phthalic anhydride) are added, and the reaction mixture is heated and boiled for 30 min at 100 °C. After 15 min, a yellow, transparent, homogeneous liquid forms. Next, when the temperature reaches 100 °C, they begin supplying nitrogen (1–2 bubbles per second) through an intermediate Soxhlett flask, making sure that the tube through which nitrogen enters the working model reaches almost to the surface of the reaction mixture. The inertness of the medium, achieved by supplying nitrogen to the system, prevents the unwanted process of gelatinization. As a result of the interaction of propylene glycol with fumaric acid and phthalic anhydride, intermediate reaction products—acid esters—are formed, which is accompanied by an increase in the temperature of the reaction mixture due to the exothermic nature of the addition process. After the temperature has stabilized and the release of water has stopped, the  $\text{ZnCl}_2$  catalyst (anhydrous) is introduced into the reaction mixture in an amount of 0.2% of the total mass of the initial reagents. In this case, the synthesis is accompanied by active mixing. Polycondensation is carried out in the temperature range 140–170 °C.

To study the polycondensation process, 30, 60, 120, and 180 min after obtaining a homogeneous mixture in the reaction flask, samples (0.3–0.4 g) were taken into pre-weighed flasks, in which the acid number and molecular weight were determined. Polycondensation was completed when the acid

number reached a value corresponding to a given molecular weight (Flynn and Wall 1966).

### Synthesis of polypropylene fumarate phthalate with acrylic acid (p-PFPh-AA)

The graft polymerization compositions were determined as p-PFPh with AA (50:50 mol%) (Burkeev et al. 2020b). The monomers mixed at this rate and the benzoyl peroxide initiator were kept in a dioxane solution, and nitrogen gas was passed for 30 min. Then, the temperature was increased to 333 K, and polymerization was started. After waiting for 52 h, the obtained grafted polymer was washed with dioxane solvent and kept in a vacuum oven until it reached a constant weight, and then the solvent and the remaining unpolymerized substances were removed.

### Synthesis of p-PFPh-AA-CPDT via RAFT polymerization technique

In addition to the amounts and techniques used in the synthesis of p-PFPh-AA, the calculated amount of CPDT (RAFT agent) was added to the medium for RAFT polymerization; the polymer solution was filled into the ampoules, and the ampoules were closed by taking them in a vacuum unit. The calculation of the concentration of the RAFT agent was introduced in accordance with previous works (Kulikov et al. 2015; Polozov et al. 2015). Nitrogen gas was passed through the ampoules for 30 min. Then, the ampoules were placed in a thermostat, and the temperature was increased up to 333 K. Next, polymerization was initiated. The polymerization time was determined as 52 h. Ampoules containing polymer solution were immersed in liquid nitrogen for the precipitation of polymers. The resulting polymers were washed with dioxane and dried in a vacuum oven until they reached a constant weight.

### Characterization

For the chemical structures of the synthesized polymers,  $^{13}\text{C}$ -NMR and  $^1\text{H}$ -NMR spectroscopy on Jeol JNN-ECA-500 using MestReNova software (version 14.2.0, Spain) were used.

PolymerLabs GPC-120 chromatography device with two Plgel columns was used for the molecular weight of the polymers. Polymers were dissolved in dioxane solvent and placed in vials, and GPC chromatograms were taken. Molecular weights and monomer conversions of the synthesized polymers were calculated by drawing a calibration graph using standard solutions with known molecular weights. Polystyrene standards were used in GPC studies.

Fourier transform infrared (FT-IR) spectra of the samples were recorded on a Thermo Scientific Nicolet iS10 FT-IR spectrometer in the wavelength range of 400–4000  $\text{cm}^{-1}$ .

The TGA study was performed by LabSYS Evo TG-dTA (Setaram, France) at a heating rate of 5°  $\text{min}^{-1}$  under an  $\text{N}_2$  atmosphere, temperature range 25–500 °C.

Equilibrium swelling of the obtained grafted polymers was achieved within 1–2 days. The degree of swelling of  $\alpha$  (%) polymers was measured gravimetrically and calculated as the ratio of the absolute mass of the swollen hydrogel at the equilibrium swell point to its initial dry mass (Burkeev et al. 2020a):

$$\alpha(\%) = \frac{m_1 - m_0}{m_0} \times 100 \quad (1)$$

where  $m_1$  and  $m_0$  are masses of swollen and dry polymer, respectively.

The morphology and architecture of the grafted polymers were studied by scanning electron microscope (SEM, JSM-7100F, JEOL, Tokyo, Japan, the accelerating voltage was 5.0 kV).

## Results and discussion

Radical graft polymerization of p-PFPh with AA is carried out at different initial mole ratios of monomers in the dioxane solution according to the following scheme shown in Fig. 1:

RAFT polymerization is characterized by the high survivability of the thiocarbonyl terminal chain for the synthesis of well-defined architectures and good control of molecular weight and molecular weight distribution of polymers.

In the study, readily available thiocarbonylthio compounds were used as chain transfer agents (RAFT agents) to give the polymerization a living character, for example, CPDT is an effective RAFT agent for both acrylates and

methacrylates (Benvenuta-Tapia et al. 2018; Chong et al. 2007, 2006; Moad et al. 2005). The scheme of the RAFT process with thiocarbonyl compounds is given in Fig. 2:

The initial oligomer polypropylene glycol fumarate phthalate was obtained by the reaction of polycondensation of propylene glycol, phthalic anhydride, and fumaric acid at temperature 503 K in the presence of aluminum chloride catalyst in an inert nitrogen medium (Burkeev et al. 2020a). When interpreting and quantitatively calculating the composition of the p-PFPh, it was taken into account that this polymer contains three groups of protons. Thus, the first group consists of =HC–CO– groups, which are components of the fumaric monomer, the second group includes –CH<sub>2</sub>–O– and –CH groups, which are parts of the structural unit of the propylene glycol monomer, and the third group is represented by the –CH<sub>3</sub> group propylene glycol component. Protons of the =HC–CO– group were detected in the region of 5–7 ppm. with integral 5.46 in the form of a singlet. <sup>1</sup>H-NMR spectra of the –CH<sub>2</sub>–O– and –CH groups appeared in the form of high-intensity multiplet signals in the region of 2–5 ppm. with an integral intensity of 4.74. The –CH<sub>3</sub> signal of the propylene glycol component appeared in the region of 0–2 ppm (doublets centered at 1.25 ppm. with 3 J 6.1 Hz, 1.19 ppm with 3 J 6.7 Hz, 1.14 ppm with 3 J 5.9 Hz, and 1.5 ppm. with 3 J 5.9 Hz with a total integrated intensity of 5.65). Minor signals in other regions of the spectrum suggest the presence of other functional groups of protic content (Fig. S1).

The presence of fumar structural groups and groups characteristic of propylene glycol in the monomer was confirmed by <sup>13</sup>C-NMR spectra. In the <sup>13</sup>C-NMR spectra, high-intensity signals of carbon atoms of the –CH<sub>3</sub> group were observed in the strong-field region of the spectrum of 10–20 ppm with an integral intensity of 14.56. Carbon atoms of –CH<sub>2</sub> and –CH groups with an integral intensity of 26.77 were manifested in the middle-field part of the spectrum of 55–75 ppm. Signals characteristic of the unsaturated bond =C–H groups in the region of 130–140 ppm were manifested with an integral

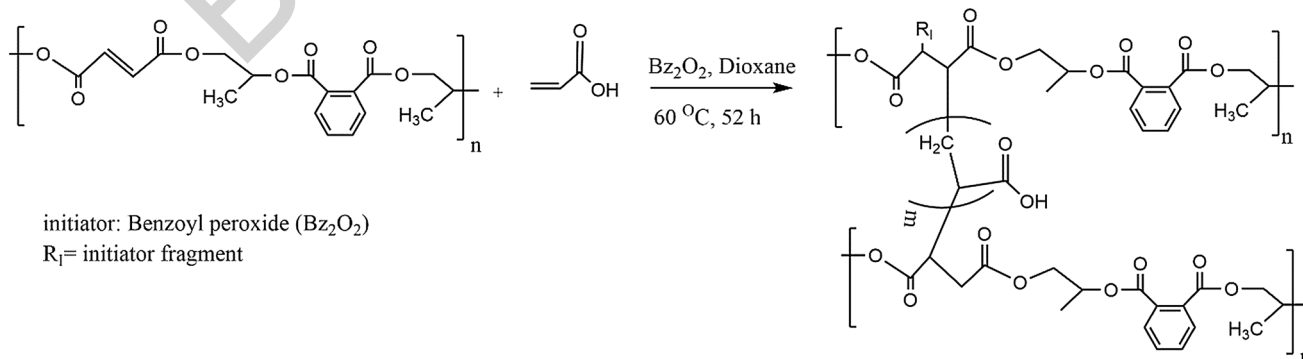


**Fig. 1** Schematic representation of radical graft polymerization of p-PFPh with acrylic acid

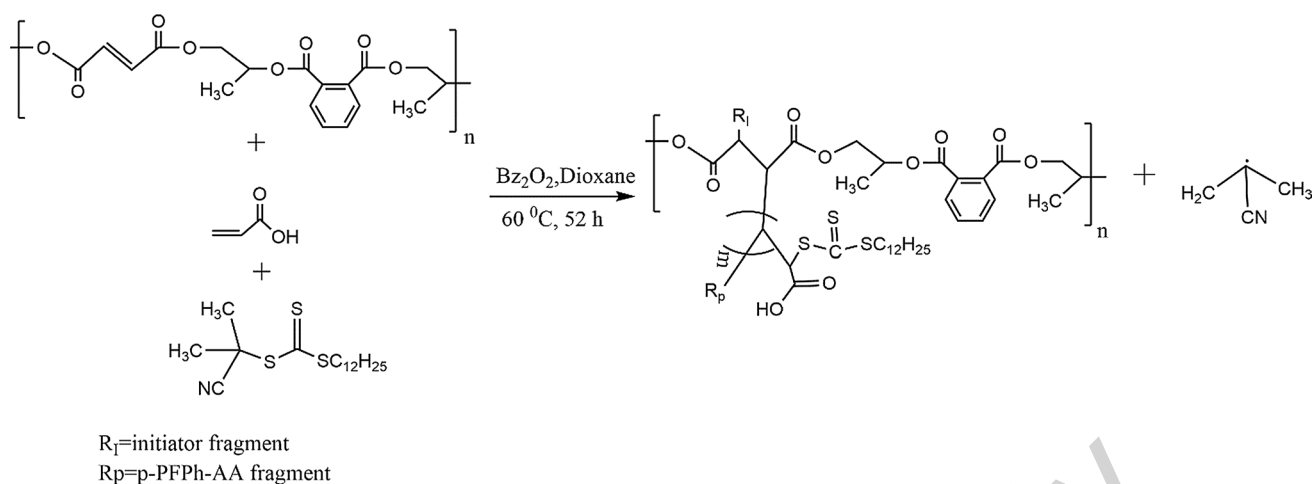


**Fig. 2** Schematic representation of the RAFT process with thiocarbonyl compounds

intensity of 20.00. In the weakest region of the spectrum at 160–170 ppm, the ester group carbons and residues of the carboxylic group of fumaric acid resonated with an integral intensity of 10.85 (Fig. S2).

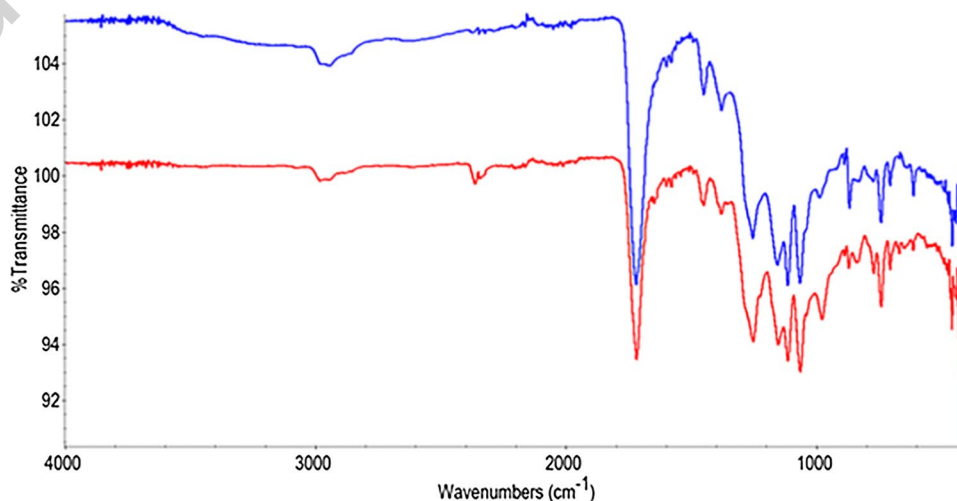
The molecular weight characteristics of the synthesized p-PFPh were studied by gel permeation chromatography (GPC), and the MW of the unsaturated polyester synthesized was found to be 1480 kDa.

In order to identify the functional bands of compounds, their FT-IR spectra were obtained. Thus, it was found that weak absorption bands in regions 2924 and 2964  $\text{cm}^{-1}$  indicated the presence of methyl groups, and wide absorption bands in region 3435  $\text{cm}^{-1}$  were characteristic of valence deviations of carboxyl functional groups. Intense absorption bands in the 1000–1200  $\text{cm}^{-1}$  region corresponded to valence deviations of the  $\text{C}-\text{O}$  polar bonds and absorption bands in the 1312 and 1373  $\text{cm}^{-1}$  regions corresponded to deviations characteristic of the  $\text{C}-\text{O}-\text{H}$  groups. Absorption

maxima of 1700  $\text{cm}^{-1}$  were characteristic of the  $\text{C}=\text{O}$  groups of the monomer molecule, and the absorption band of 2800–2400  $\text{cm}^{-1}$  indicated the OH acid group. The absence of intense bands in the 1640  $\text{cm}^{-1}$  region in the p-PFPh spectra indicated the formation of a network structure of grafted polymers, accompanied by a break in unsaturated bonds  $\text{C}=\text{C}$  (Fig. 3.).

It should also be noted that when the obtained FT-IR spectrum of the p-PFPh/AA/CPDT grafted polymer shown in Fig. 3 is analyzed, there are signals in the 3025  $\text{cm}^{-1}$  region characteristics of  $\text{C}-\text{H}$  of aromatic hydrocarbon group, 2920  $\text{cm}^{-1}$  and 2850  $\text{cm}^{-1}$  for  $\text{C}-\text{H}_3$ ,  $\text{C}-\text{H}_2$  and  $\text{C}-\text{H}$  groups of aliphatic hydrocarbon, 2260  $\text{cm}^{-1}$  for  $\text{C}-\text{N}$  group, 1730  $\text{cm}^{-1}$  for  $\text{C}=\text{O}$  group, as well as 1490  $\text{cm}^{-1}$  for the group  $\text{C}=\text{C}$  aromatic hydrocarbon, 1150  $\text{cm}^{-1}$  for  $\text{C}-\text{O}$ ,  $\text{C}=\text{S}$  stretching at 1450  $\text{cm}^{-1}$ , 1059  $\text{cm}^{-1}$ , and 757  $\text{cm}^{-1}$ , in good agreement with the observed values of 1417  $\text{cm}^{-1}$ , 1083  $\text{cm}^{-1}$ , and 730  $\text{cm}^{-1}$  and 1070  $\text{cm}^{-1}$

**Fig. 3** FT-IR spectra of p-PFPh:AA (blue line), p-PFPh:AA:CPDT (red line)



for –SC groups (Wiles et al. 1966). However, it is worth noting that in general the IR spectra of the p-PFPh/AA and p-PFPh/AA/CPDT grafted polymers have identical curves, but it indicates the presence of stretching signals cyano and C=S.

Surface morphology of p-PFPh:AA and p-PFPh:AA:CPDT grafted polymers was studied by SEM. The results are shown in Fig. 4. On the micrograph (Fig. 4a), it is observed that the surfaces of the particles of p-PFPh:AA samples (a) have hard and brittle cleavage sites. In the course of microanalysis, the p-PFPh:AA:CPDT grafted polymers (b) show signs of a loose surface and the formation of a layered and porous structure in comparison with the grafted polymers. In addition, the analysis revealed pores. It is evident from the SEM topography that an increase in the concentration of the RAFT agent leads to the formation of a network and affects the sizes of the formed pores (since the RAFT technique provides significant superiority in the control of polymer chains, it enables the adjustment of network

structure and pore states), which give a high swelling capacity to the polymers (Fig. 4b).

Thus, we synthesized a number of p-PFPh-AA-CPDT grafted polymers at different molar ratios [BP]:[CPDT]. The results of the study are shown in Table 1. The polymers obtained as a result of polymer synthesis are crosslinked p-PFPh-AA (product 1) and p-PFPh-AA-CPDT-based branched polymer (product 2), respectively, with a porous structure. As can be seen in Table 1, it is found that the swelling capacity increases branchedly with increasing CPDT concentration. The same p-PFPh-containing polymers significantly increased the swelling capacity by increasing the CPDT concentration in the starting polymer–monomer mixture and allowed a polymer to obtain a more flexible structure. It is also worth noting that as the CPDT content increases, so does the yield of product 2.

In the continuation of the study, the bromine number and the degree of unsaturation of the synthesized grafted polymers were determined. The results are shown in Table 2.

**Fig. 4** Surface morphology of **a** p-PFPh:AA and **b** p-PFPh:AA:CPDT

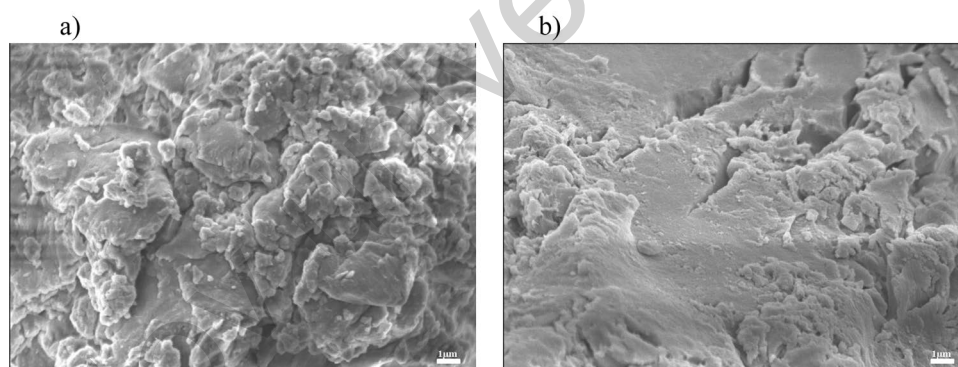


**Table 1** Effect of RAFT agent concentration on p-PFPh/AA graft polymerization mechanism in dioxane solution

Concentration of RAFT, [CPDT] = 10 <sup>3</sup>	Crosslinked polymer			Branched polymer	
	Yield, %	[m <sub>1</sub> ]:[m <sub>2</sub> ] Mol. %	Swelling, α, %	Yield, %	[m <sub>1</sub> ]:[m <sub>2</sub> ] Mol. %
–	89.33	48.58:51.42	115.34	–	–
20	78.21	47.37:52.63	332.41	21.18	32.45:67.55
40	42.62	46.28:53.72	442.26	57.38	37.16:63.84
60	12.84	45.13:54.87	526.23	87.42	44.67:55.33

Polymerization Conditions: T = 70 °C, [I] = 8 × 10<sup>−3</sup> mol/L, [M<sub>1</sub> + M<sub>2</sub>] = 1.5 × 10<sup>−3</sup> + 1.5 × 10<sup>−3</sup> mol/L

**Table 2** Effect of RAFT agent concentration on p-PFPh/AA graft polymerization mechanism in dioxane solution

Concentration of RAFT, 10 <sup>3</sup>	B.N. crosslinked	B.N. branched	Degree of unsaturation crosslinked	Degree of unsaturation branched
–	15.42	–	56.23	–
20	14.23	24.72	40.19	76.17
40	12.74	25.14	34.16	81.12
60	11.06	27.23	28.84	91.86

Reaction conditions, t = 70 °C, [M<sub>1</sub> + M<sub>2</sub>] = 1.5 × 10<sup>−3</sup> + 1.5 × 10<sup>−3</sup> mol/L

As can be seen from Table 2, as the CPDT content of the starting polymer–monomer mixture increases, the unsaturation of the p-PFPh-AA grafted polymer of the polymer-based mesh structure decreases, while the inverse relationship is observed for the p-PFPh-AA grafted polymer of the branched structure.

To evaluate the chemical compositions of polymers and their degree of purity, a thermal analysis of the samples was carried out: p-PFPh-AA with CPDT agent and p-PFPh-AA (Fig. 5).

In particular, the changes in TGA graphs observed as a result of grafting the AA used in this study onto different polymer types are available in the literature (Burkeev et al. 2013, 2015a, 2015b). The changes observed in this study are compatible with the literature, and changes in some parameters were detected due to the polymer type. During thermogravimetric analysis, the determined thermal stability parameters of the p-PFPh-AA grafted polymer were compared with the p-PFPh-AA polymer in the presence of a CPDT agent. Thermogravimetric curves (mass changes and mass loss rate from temperature) are shown in Fig. 5. As can be seen, thermograms have a similar

character, which suggests a similar mechanism of polymer behavior during degradation. It was found that for both grafted polymers, p-PFPh-AA, and p-PFPh-AA with a CPDT agent, dTG analysis showed the presence of single degradation peaks. The most intensive degradation of the crosslinked p-PFPh-AA polymer with the CPDT agent, associated with the cleavage of the main macromolecular chain (accompanied by the release of gaseous products), and the final degradation of the polymer, takes place in the 314–434 °C temperature region, as evidenced by the characteristic peaks in the dTG curves (Fig. 5b) with a maximum  $T_{\max} = 344$  °C at a heating rate of 5 °C min<sup>-1</sup>. The p-PFPh-AA-based mesh polymer (Figs. 5c and d) shows a peak with a maximum of  $T_{\max} = 330$  °C in this region. However, in both cases, especially at lower heating rates, a small shoulder or even a second decomposition peak was observed at lower temperatures, ranging from 30 to 200 °C. These data confirm that the mechanism of thermal decomposition of grafted polymers, p-PFPh-AA, and p-PFPh-AA with the CPDT agent is quite complex, thus it involves the decomposition of the ester group followed by thermal decomposition of the backbone.

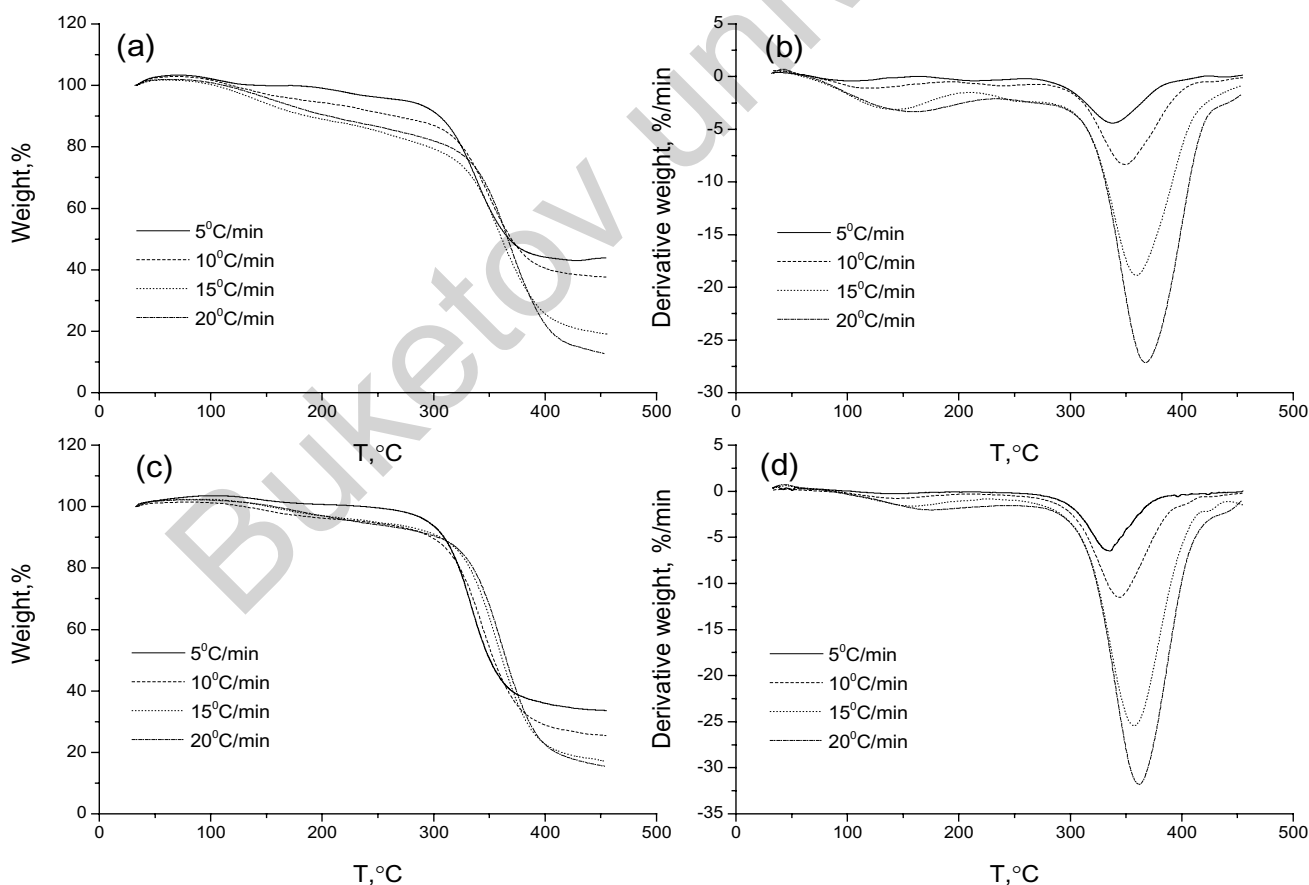


**Fig. 5** Temperature Relationships of Mass Change (TG Curve), Mass Change Rate (dTG Curve) for Crosslinked p-PFPh-AA Polymer with CPDT Agent (a and b), and p-PFPh-AA Polymer (c and d)

Using the data from the experiments performed (Fig. 5), Friedman, Ozawa–Flynn–Wall (Friedman 1964; Flynn and Wall 1966) evaluated the activation energies of chemical transformation during the degradation of the p-PFPh-AA polymer and crosslinked p-PFPh-AA polymer with the CPDT agent. A graphical interpretation of the Friedman, Ozawa–Flynn–Wall (Friedman 1964; Flynn and Wall 1966) methods is shown in Figs. 5 and 6. The values of the kinetic parameters of thermal destruction for one-stage processes are determined by the rate of change in the mass of the sample:  $-\frac{dw}{dt} = A \exp\left(-\frac{E}{RT}\right)$ . Since it is analytically impossible to solve the right side of the equation, various approximate methods are used in practice (Fig. 6).

For the simplest isoconversion methods, the activation energy is determined by the slope of the portion by two parameters, which are determined by  $T, \alpha$ , and  $\beta$ . We will call them direct isoconversion methods. One of these methods is the method obtained by the differential Friedman method (Fig. 6a and c). By measuring the temperature at different

heating rates (5.0–20.00 °C min<sup>-1</sup>) and the  $d\alpha/dT\alpha$  conversion rate at a fixed stage for each of the experiments, we can obtain  $E$  from the slope of the  $\ln$  sections ( $\beta \cdot d\alpha/dT\alpha$ ) from the  $1000/T$ . Ozawa–Flynn–Wall proposed a method for determining the value of thermolysis activation energy at different heating rates, at which  $E$  is determined by the slope of the  $\ln\beta$  sections from the  $1000/T$  (Fig. 6b and d). It is clear that a wide range of isoconversion techniques can be obtained by applying different approximations.

The reliability of these methods is similar, and they are simple and convenient although the Ozawa–Flynn–Wall (OFW) method has a slight advantage in that each axis of the section uses only one variable (Fig. 7, Table 3). Friedman's method does not use mathematical approximation but instead uses the definition of the reaction rate at the equivalent reaction stage for different heating rates.

Analysis of thermogravimetric measurements (Fig. 7, Table 3) shows that both the composition and, most importantly, the sequence of monomer units along the grafted polymer chain plays an important role in determining the

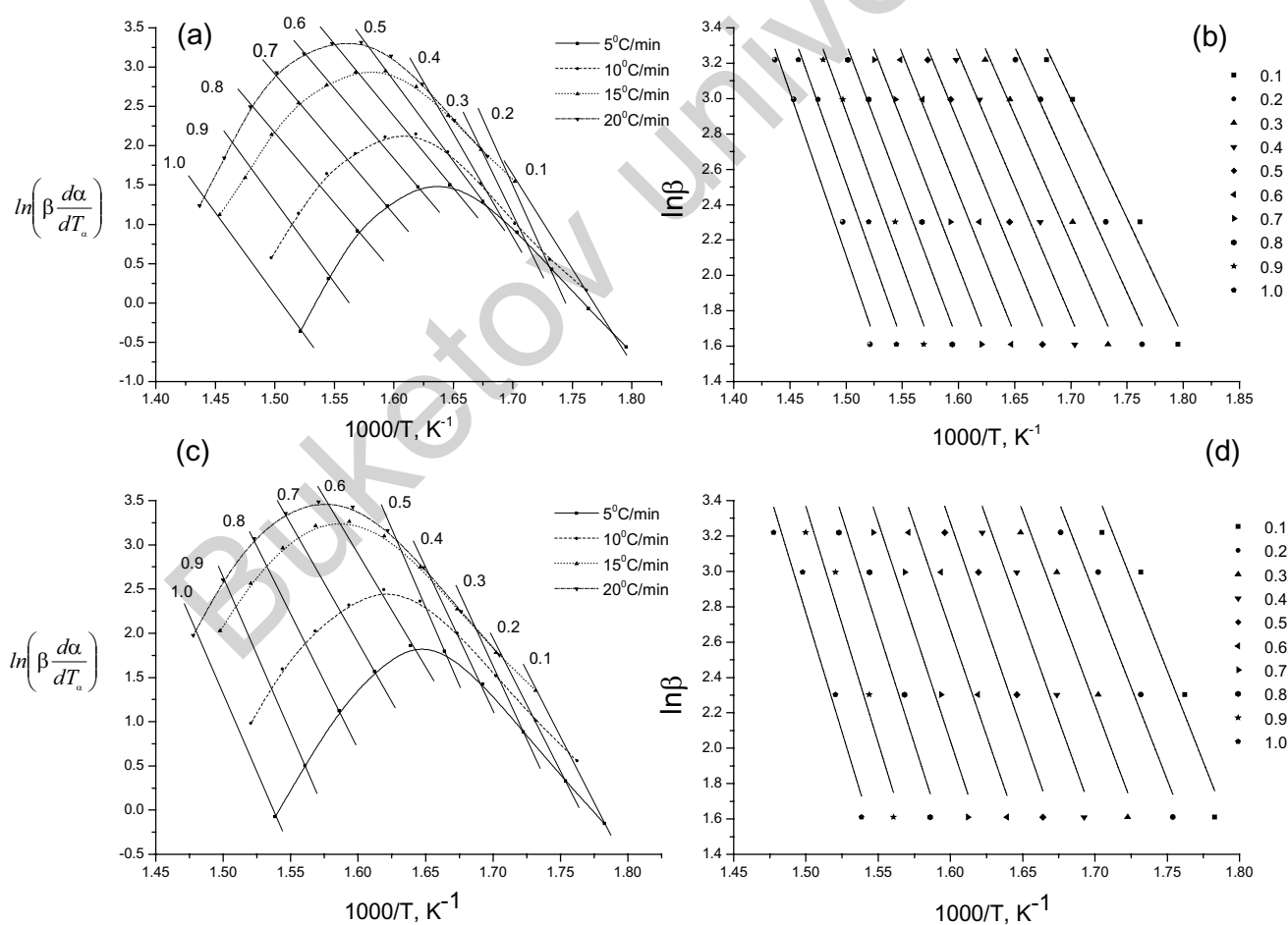


**Fig. 6** Graphical Analysis Results Determined by Friedman, Ozawa–Flynn–Wall Methods for Crosslinked p-PFPh-AA with CPDT Agent (**a** and **b**) and p-PFPh-AA-based mesh polymer (**c** and **d**) at Heating Rates 5.0–20.00 °C/min

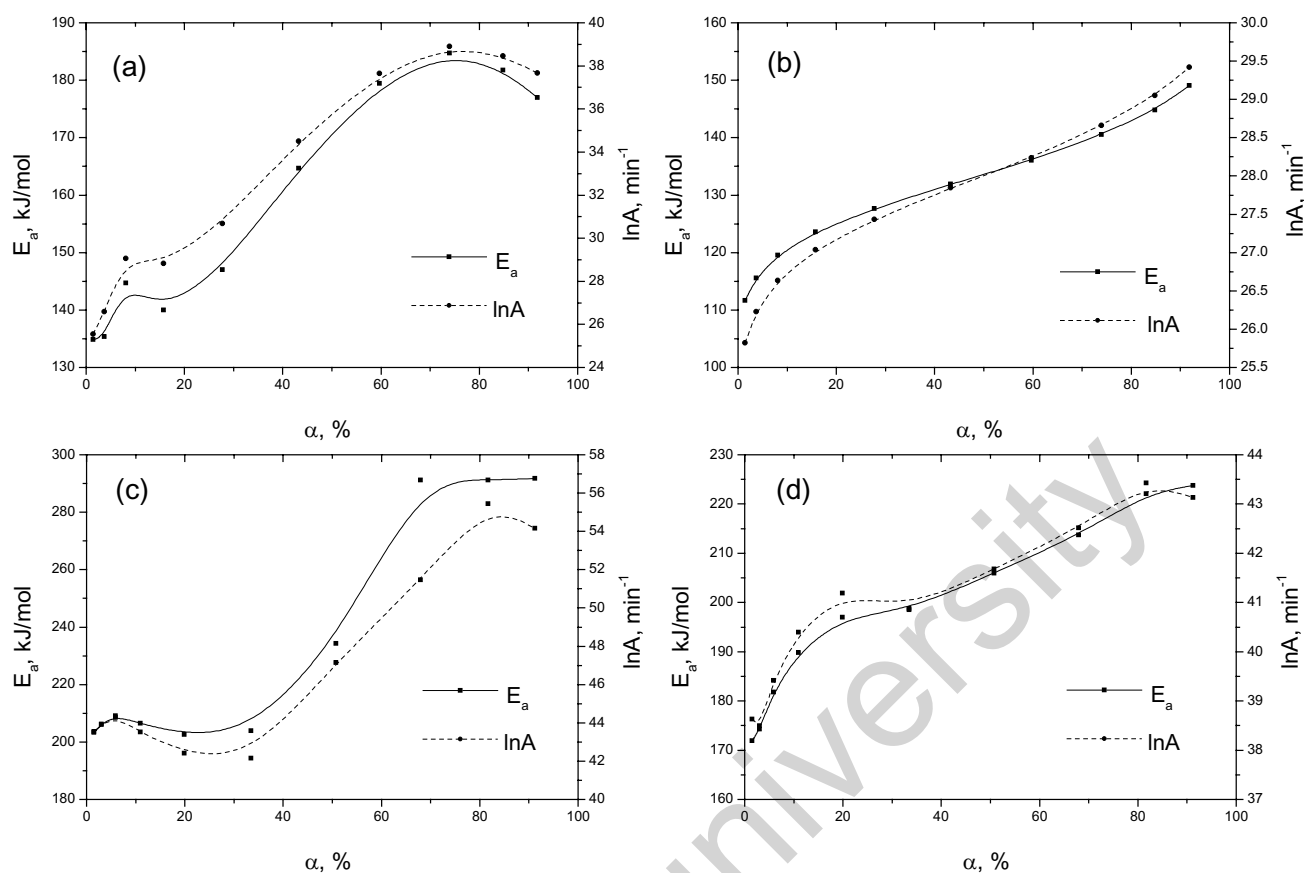


**Fig. 7** Activation energy and pre-exponential factor as a function of partial peak area for a crosslinked p-PFPh-AA polymer with CPDT agent (a and b) and p-PFPh-AA-based mesh polymer (c and d)

thermal decomposition kinetics of the grafted polymers. As can be seen from Fig. 7, at different heating rates from 5.0 to 20.00 °C min<sup>-1</sup>, the obtained average activation energy

**Table 3** Activation energy by FR and OFW for crosslinked polymer p-PFPh-AA and with CPDT agent

Transformation, $\alpha$	FR		OFW	
	p-PFPh-AA	p-PFPh-AA with CPDT	p-PFPh-AA	p-PFPh-AA with CPDT
0.1	203.23 ± 4	134.86 ± 5	174.24 ± 4	111.62 ± 5
0.2	206.18 ± 4	135.35 ± 5	181.81 ± 4	115.57 ± 5
0.3	209.09 ± 4	144.71 ± 5	189.80 ± 4	119.55 ± 5
0.4	206.45 ± 4	139.95 ± 5	197.02 ± 4	123.61 ± 5
0.5	202.57 ± 4	147.02 ± 5	198.52 ± 4	127.67 ± 5
0.6	203.92 ± 4	164.70 ± 5	205.96 ± 4	131.89 ± 5
0.7	234.29 ± 4	179.39 ± 5	213.72 ± 4	136.06 ± 5
0.8	291.13 ± 4	184.73 ± 5	222.04 ± 4	140.50 ± 5
0.9	291.73 ± 4	176.97 ± 5	223.74 ± 4	149.07 ± 5

Reaction conditions,  $t = 70$  °C,  $[M_1 + M_2] = 1.5 \times 10^{-3} + 1.5 \times 10^{-3}$  mol/L

and pre-exponential factor data are reduced in the order of FR (= 159.00 kJ mol<sup>-1</sup>) > OFW (= 130.04 kJ mol<sup>-1</sup>) methods for the crosslinked p-PFPh-AA polymer with CPDT agent, and the p-PFPh-AA-based mesh polymer FR (= 234.00 kJ mol<sup>-1</sup>) > 198.00 Comparing data from the Friedman, Ozawa–Flynn–Wall approaches, it is clear that the results on activation energies are in close proximity. However, the first method gives  $E_a$  values 10–20% lower than that of the program organizational unit (POU) method. This is reasonable because these methods are based on relatively different approximations. However, it is believed that the FR equation provides more reliable and accurate results compared to the OFW equation.

## Conclusions

The initial oligomer polypropylene glycol fumarate phthalate was obtained by the polycondensation reaction of propylene glycol, phthalic anhydride, and fumaric acid at a temperature of 503 K in the presence of an aluminum chloride catalyst in an inert nitrogen medium. The presence of fumaric

structural groups and the group's characteristic of propylene glycol in the monomer were confirmed by  $^1\text{H-NMR}$  and  $^{13}\text{C-NMR}$  spectra. By GPC, the MW of the polypropylene fumarate phthalate synthesized was found 1480 kDa. Polypropylene fumarate phthalate reacts in radical graft polymerization with acrylic acid to form polymers with a network structure. It is assumed that the addition of a RAFT agent to these systems allows changing the reaction mechanism, thereby forming two products as a result of the reaction: a crosslinked graft polymer and a soluble branched polymer. Analysis of crosslinked polymer samples by FT-IR spectrometer is identical in the nature of the curves, indicating the same type of crosslinking formation. At the same time, differences were observed in the SEM images of the hydrogels in order to study the effect of the RAFT agent. Morphological changes were studied as a result of the change of the mechanism with the addition of the RAFT agent to the medium. Activation energies and thermodynamic parameters were calculated in light of detailed thermogravimetric analyses. As a result, due to the change of the mechanism of such grafted polymer systems under the influence of the RAFT agent, very promising results have been reported in obtaining new-generation products with high controllable swelling capacity and polymer yielding.

**Supplementary Information** The online version contains supplementary material available at <https://doi.org/10.1007/s11696-024-03354-0>.

**Acknowledgements** This research has been funded by the Science Committee of the Ministry of Education and Science of the Republic of Kazakhstan (Grant № AP15473241). The authors would like to thank Gazi University Academic Writing Application and Research Center for proofreading the article.

**Author contributions** ZG, SA, and YT contributed to conceptualization; ZG, SA, YT, and GK provided methodology; ZG and EY performed visualization and writing—original draft; ZG, EY, SA, YT, and GK performed writing—review and editing.

**Data availability** Data will be made available on request.

## Declarations

**Conflict of interest** The authors declare that they have no known competing financial interests or personal relationships that could have appeared to influence the work reported in this paper.

**Open Access** This article is licensed under a Creative Commons Attribution 4.0 International License, which permits use, sharing, adaptation, distribution and reproduction in any medium or format, as long as you give appropriate credit to the original author(s) and the source, provide a link to the Creative Commons licence, and indicate if changes were made. The images or other third party material in this article are included in the article's Creative Commons licence, unless indicated otherwise in a credit line to the material. If material is not included in the article's Creative Commons licence and your intended use is not permitted by statutory regulation or exceeds the permitted use, you will need to obtain permission directly from the copyright holder. To view a copy of this licence, visit <http://creativecommons.org/licenses/by/4.0/>.

## References

- Abbasian M, Amirmanesh M (2017) Polymerically modified clays to preparation of polystyrene nanocomposite by nitroxidemediated radical polymerization and solution blending methods. *Polym Compos* 38(6):1127–1134
- Abbasian M, Khakpour AN (2016) Nitroxide-mediated radical polymerization of styrene initiated from the surface of titanium oxide nanoparticles. *J Nanostruct* 6(1):38–45
- Abbasian M, Khakpour AN, Shoja ES (2013) Synthesis of poly (methyl methacrylate)/zinc oxide nanocomposite with core-shell morphology by atom transfer radical polymerization. *J Macromol Sci Part A* 50(9):966–975
- Abbasian M, Massomi B, Rashidzadeh B, Bahrami H (2015) Versatile method for synthesis of electrically conductive polypyrrole polystyrene clay nanocomposites using ATRP and chemical polymerization methods. *J Exp Nanosci* 10(11):844–858
- Ageyeva T, Sibikin I, Karger-Kocsis J (2018) Polymers and related composites via anionic ring-opening polymerization of lactams: recent developments and future trends. *Polymers* 10(4):357
- Ahmadvani L, Abbasian M, Akbarzadeh A (2017) Synthesis of sharply thermo and PH responsive PMA-b-PNIPAM-b-PEG-b-PNIPAM-b-PMA by RAFT radical polymerization and its schizophrenic micellization in aqueous solutions. *Des Monomers Polym* 20:406–418
- Barner-Kowollik C (2008) Handbook of RAFT polymerization. Wiley-VCH, Weinheim
- Baskaran R, Sarojadevi M, Vijayakumar CT (2011) Unsaturated polyester nanocomposites filled with nano alumina. *J Mater Sci* 46:4864–4871
- Benvenuta-Tapia JJ, Tenorio-Lopez JA, Vivaldo-Lima E (2018) Estimation of reactivity ratios in the raft copolymerization of styrene and glycidyl methacrylate. *Macromol React Eng* 12(5):1800003
- Burkeev MZh, Magzumova AK, Tazhbaev EM, Burkeeva GK, Kovaleva AK (2013) Effect of external factors on the swelling of hydrogels based on poly(ethylene glycol) maleate with some vinyl monomers. *Russ J Appl Chem* 86(1):63–68
- Burkeev MZh, Kovaleva AK, Tazhbaev EM, Burkeeva GK, Davrenbekov SZh et al (2015a) Nanocatalytic systems based on poly(ethylene glycol maleate)-acrylamide copolymers. *Russ J Appl Chem* 88(2):313–319
- Burkeev MZh, Sarsenbekova AZh, Figurinene SN (2015b) Thermal destruction of copolymers of polypropylene glycol maleate with acrylic acid. *Russ J of Phys Chem* 89:2183–2189
- Burkeev MZh, Kudaibergen GK, Burkeeva GK et al (2018) New Polyampholyte polymers based on polypropylene glycol fumarate with acrylic acid and dimethylaminoethyl methacrylate. *Russ J Appl Chem* 91:1145–1152
- Burkeev MZh, Zhumanazarova GM, Tazhbayev EM, Kudaibergen GK, Aukadiyeva SB, Zhakupbekova EZ (2020a) Poly(propylene fumarate phthalate) and acrylic acid radical copolymerization constants and parameters. *Bull Univ Karaganda Chem* 97(1):68–74
- Burkeev MZh, Zhumanazarova GM, Tazhbayev EM, Kudaibergen GK, Turlybek GA, Zhakupbekova EZ (2020b) Research of the influence of external factors on copolymers based on unsaturated polyester resins. *Bull Univ Karaganda Chem* 98(2):51–57
- Burkeev MZh, Bolatbay AN, Sarsenbekova AZh, Davrenbekov SZh, Nasikhatuly E (2021a) Integral ways of calculating the destruction of copolymers of polyethylene glycol fumarate with acrylic acid. *Russ J Phys Chem* 95:2009–2013
- Burkeev MZ, Shibaeva SR, Khamitova TO, Plocek J, Tazhbayev YM, Davrenbekov SZ, Nurmaganbetova MT, Kazhmuratova AT, Zhumagalieva TS, Kezdikbayeva AT (2021b) Synthesis and catalytic properties of new polymeric monometallic composites based on copolymers of polypropylene glycol maleate phthalate

- with acrylic acid. *Polymers* 13(24):4369. <https://doi.org/10.3390/polym13244369>
- Burkeev MZ, Zhunisova MS, Tazhbayev YM, Fomin VN, Sarsenbekova AZh et al (2022) Influence of RAFT agent on the mechanism of copolymerization of polypropylene glycol maleinate with acrylic acid. *Polymers* 14(9):1884
- Chat K, Maksym P, Kaminski K, Adrjanowicz K (2022) Stereoregulation, molecular weight, and dispersity control of PMMA synthesized via free-radical polymerization supported by the external high electric field. *Chem Commun* 58:5653–5656
- Chen ZW, Yu Y, Zhang QW, Chen TT, Jiang JC (2019) Preparation of phosphorylated chitosan-coated carbon microspheres as flame retardant and its application in unsaturated polyester resin. *Polym Adv Technol* 30:1–10
- Chong B, Moad G, Rizzardo E, Skidmore M, Thang SH (2006) Thermolysis of RAFT-synthesized poly(methyl methacrylate). *Aust J Chem* 59(10):755–762
- Chong YK, Moad G, Rizzardo E, Thang SH (2007) Thiocarbonylthio end group removal from RAFT-synthesized polymers by radical-induced reduction. *Macromolecules* 40(13):4446–4455
- Clothier GKK, Guimarães TR, Thompson SW et al (2023) Multiblock copolymer synthesis via RAFT emulsion polymerization. *Chem Soc Rev* 52(10):3438–3469. <https://doi.org/10.1039/d2cs00115b>
- Czajka A, Lovell PA, Armes SP (2022) Time-resolved small-angle X-ray scattering studies during the aqueous emulsion polymerization of methyl methacrylate. *Macromolecules* 143(3):1474–1484
- Flynn JH, Wall LA (1966) A quick, direct method for the determination of activation energy from thermogravimetric data. *Polym Lett* 4(5):323–328
- Formela K, Kurańska M, Barczewski M (2022) Recent advances in development of waste-based polymer materials: a review. *Polymers* 14(5):1050
- Friedman HL (1964) Kinetics of thermal degradation of char-forming plastics from thermogravimetry. Application to a phenolic plastic. *J Polym Sci Part C* 6(1):183–195
- György C, Armes SP (2023) Recent advances in polymerization-induced self-assembly (PISA) syntheses in non-polar media. *Angew Chem Int Ed Engl* 62(42):e202308372. <https://doi.org/10.1002/anie.202308372>
- Heiny M, Shastri VP (2015) Cyclic comonomers for the synthesis of carboxylic acid and amine functionalized poly(l-lactic acid). *Molecules* 20(3):4764–4779
- IriSofa S, Abbasian M, Mirzaei M (2019) Synthesis and micellar characterization of novel pH-sensitive thiol-ended triblock copolymer via combination of RAFT and ROP processes. *Int J Polym Mater Polym Biomater* 68(6):297–307
- Kandelbauer A, Tondi G, Goodman SH (2014) Unsaturated polyesters and vinyl esters. In: Dodduk H, Goodman SH (eds) *Handbook of thermoset plastics*, 3rd edn. William Andrew Publications, San Diego
- Karaj-Abad GS, Abbasian M, Jaymand M (2019) Nitroxidemediated graft copolymerization of styrene from cellulose and its polymer/montmorillonite nanocomposite. *J Elastomers Plast* 51(5):473–489
- Kazhmuratova AT, Zhunisova MS, Plocek J, Fomin VN, Sarsenbekova AZh, Khamitova TO (2022) Influence of the RAFT agent on the reaction direction of the copolymerization of polypropylene glycol maleate with acrylic acid. *Bull Univ Karaganda Chem* 107(3):189–197
- Kulikov EE, Zaitsev SD, Semchikov YD (2015) Reversible addition-fragmentation chain transfer (RAFT) (Co)polymerization of isobornyl acrylate. *Polym Sci Ser C* 57:120–127
- Lee KM, Kim KH, Yoon H, Kim H (2018) Chemical design of functional polymer structures for biosensors: from nanoscale to macroscale. *Polymers* 10(5):551
- Liu LC, Wang GX, Wu H, Lu M (2013) Activators regenerated by electron transfer in ATRP of methyl methacrylate with alcohol as reducing agent in the presence of a base. *Iran Polym J* 22:891–896
- Mahmoodzadeh F, Abbasian M, Jaymand M, Amirshaghghi A (2017) A novel dual stimuli-responsive thiol-end-capped ABC triblock copolymer: synthesis via reversible addition-fragmentation chain transfer technique, and investigation of its self-assembly behavior. *Polym Int* 66(11):1651–1661
- Moad G (2015) RAFT polymerization—then and now. *ACS Symp Ser* 1187:211–246
- Moad G, Chong Y, Postma A, Rizzardo E, Thang SH (2005) Advances in RAFT polymerization: the synthesis of polymers with defined end-groups. *Polymer* 46(19):8458–8468
- Moad G, Rizzardo E, Thang SH (2013) RAFT polymerization and some of its applications. *Chem Asian J* 8(8):1634–1644
- Mohammad-Rezaei R, Massoumi B, Abbasian M, Jaymand M (2018) Novel strategies for the synthesis of hydroxylated and carboxylated polystyrenes. *J Polym Res* 25:93
- Munyati MO, Lovell PA (2007) Preparation, morphology and thermal properties of rubber-modified polyester resins. *E Polym* 7(1):052
- Muringayil Joseph T, Murali Nair S, Kattimuttathu Ittara S, Haponiuk JT, Thomas S (2020) Copolymerization of styrene and pentadecylphenylmethacrylate (PDPMA): synthesis, characterization, thermomechanical and adhesion properties. *Polymers* 12(1):97. <https://doi.org/10.3390/polym12010097>
- Naguib HM, Zhang XH (2018) Advanced recycled polyester based on PET and oleic acid. *Polym Test* 69:450–455
- Odian G (2004) *Principles of polymerization*, 4th edn. John Wiley & Sons, Hoboken, p 835
- Polozov EY, Zaitsev SD, Semchikov YD (2015) Low-temperature reversible addition-fragmentation chain transfer (RAFT) polymerization of methyl methacrylate. *Russ J Appl Chem* 87:1294–1299
- Sarsenbekova AZh, Kudaibergen GK, Burkeev MZ, Burkeeva GK (2019) Comparative analysis of the thermal decomposition kinetics of polyethylene glycol fumarate-acrylic acid copolymers. *Russ J Phys Chem* 93:1252–1257
- Sarsenbekova AZ, Zhumanazarova GM, Tazhbayev YM, Kudaibergen GK, Kabieva SK, Issina ZA, Kaldybayeva AK, Mukabylova AO, Kilybay MA (2023) Research the thermal decomposition processes of copolymers based on polypropyleneglycolfumaratephthalate with acrylic acid. *Polymers* 15(7):1725
- Suresh KI, Nutenki R, Joseph TM, Murali S (2022) Structural, molecular and thermal properties of cardanol based monomers and polymers synthesized via atom transfer radical polymerization (ATRP). *J Macromol Sci Part A* 59(6):403–410. <https://doi.org/10.1080/10601325.2022.2053288>
- Tanaka J, Archer NE, Grant MJ, You W (2021) Reversible-addition fragmentation chain transfer step-growth polymerization. *J Am Chem Soc* 143(39):15918–15923
- Tanaka J, Li J, Clouthier SM, You W (2023) Step-growth polymerization by the RAFT process. *Chem Commun (Camb)* 59(53):8168–8189. <https://doi.org/10.1039/d3cc01087b>
- Tardy A, Nicolas J, Gimes D, Lefay C, Guillaneuf Y (2017) Radical ring-opening polymerization: scope, limitations, and application to (bio)degradable materials. *Chem Rev* 117(3):1319–1406
- Tian XY, Ding JJ, Zhang B, Qiu F, Zhuang XD, Chen Y (2018) Recent advances in RAFT polymerization: novel initiation mechanisms and optoelectronic applications. *Polymers* 10(3):318
- Truong NP, Jones GR, Bradford KGE, Konkolewicz D, Anastasaki A (2021) A comparison of RAFT and ATRP methods for controlled radical polymerization. *Nat Rev Chem* 5:859–869
- Van Steenberghe PHM, Sedlacek O, Hernandez-Ortiz JC, Verbraeken B, Reyniers MF, Hoogenboom R, D'hooge DR (2019) Visualization and design of the functional group distribution during statistical copolymerization. *Nat Commun* 10(1):3641

- Wiles DAI, Gingskas BA, Suprlinchuk T (1966) The C=S stretching vibration in the infrared spectra of some thiosemicarbazones. *Can J Chem* 45(5):466–473
- Xie WS, Zhao LY, Wei Y, Yuan JY (2021) Advances in enzyme-catalysis-mediated RAFT polymerization. *Cell Rep Phys Sci* 2(7):100487
- Yasko AW, He S, Engel PS, Yaszemski JM, Mikos AG (2000) Injectable biodegradable polymer composites based on poly(propylenefumarate) with poly(ethylene glycol)-dimethacrylate. *Biomaterials* 21(23):2389–2394
- Zhao D, Wang J, Wang XL, Wang YZ (2018) Highly thermostable and durably flame-retardant unsaturated polyester modified by a novel polymeric flame retardant containing Schiff base and spirocyclic structures. *Chem Eng J* 344:419–430
- Zhou MJ, He F, Wu H, Wang GX, Liu LC, Xu W (2019) Photoinduced ATRP of MMA without ligands in ionic liquid. *Iran Polym J* 26:10

**Publisher's Note** Springer Nature remains neutral with regard to jurisdictional claims in published maps and institutional affiliations.

Buketov university